NANO LETTERS

2005
Vol. 5, No. 5
925−929

Enumeration of DNA Molecules Bound to a Nanomechanical Oscillator

B. Ilic,*,† Y. Yang,† K. Aubin,† R. Reichenbach,‡ S. Krylov,§ and H. G. Craighead†

School of Applied and Engineering Physics, Nanobiotechnology Center and Cornell Nanofabrication Facility, Cornell University, School of Electrical and Computer Engineering, Cornell University, and Department of Solid Mechanics Materials and Systems, Tel Aviv University 69978 Ramat Aviv, Israel

Received March 9, 2005; Revised Manuscript Received April 7, 2005

ABSTRACT

Resonant nanoelectromechanical systems (NEMS) are being actively investigated as sensitive mass detectors for applications such as chemical and biological sensing. We demonstrate that highly uniform arrays of nanomechanical resonators can be used to detect the binding of individual DNA molecules through resonant frequency shifts resulting from the added mass of bound analyte. Localized binding sites created with gold nanodots create a calibrated response with sufficient sensitivity and accuracy to count small numbers of bound molecules. The amount of nonspecifically bound material from solution, a fundamental issue in any ultra-sensitive assay, was measured to be less than the mass of one DNA molecule, allowing us to detect a single 1587 bp DNA molecule.

The drive toward ultrasensitive biochemical assays has motivated significant efforts in single molecule detection and identification.[1−7] Resonant nanomechanical devices[8−13] provide an alternative approach to techniques such as those using fluorescent labels.[14,15] The mechanical approaches also have the possibility of quantification of the bound molecules, and can be incorporated in array-based systems for multiplexed biochemical analyses. Carbon nanotubes, attractive because of their uniform diameters and small mass,[16−19] have also been considered as biomolecular detectors, but remain difficult to incorporate in device architectures and have not yet been able to quantify specifically bound biomolecules.

We have detected the binding of functionalized 1578 base pair long double-stranded deoxyribonucleic acid (dsDNA) molecules to nanomechanical oscillators by measuring the resonant frequency shift due to the added mass of the bound molecules. The binding of a single DNA molecule could readily be detected. The resonant frequency of individual oscillators in an array of resonator devices was measured by thermooptically driving the individual devices and detecting their motion by optical interference. The number of bound molecules on each device was quantified as proportional to the measured frequency shift with a proportionality constant determined experimentally and verified by modeling of the mechanical response of the system. For the smallest and most sensitive cantilevers the mass sensitivity was 194 Hz/attogram. The resonant frequency shift of the oscillators can be measured with high accuracy, having a practical experimental uncertainty of ∼10 Hz corresponding to ∼0.05ag. The nonspecific binding of material to the oscillator throughout the process, however, limits the quantification of the specifically bound compounds for a particular analytical process. We measured the effects of nonspecific binding of material other than the DNA from our solutions and found this to be approximately 0.43 ± 0.23ag for an oscillator of length $l = 3.5\mu$m, with 0.23ag therefore being the approximate limiting mass resolution resulting from uncontrolled binding to the surface in our particular process. For the smallest ($l = 3.5\mu$m), most sensitive oscillator this mass uncertainty corresponds to the mass of ∼0.26 DNA molecules, enabling us to be able to resolve a single molecule. With the most sensitive devices and dilute DNA concentrations, we have detected a single dsDNA molecule.

Our devices were fabricated from 90 nm thick low-pressure chemical vapor deposited low-stress silicon nitride in conjunction with a thermally grown sacrificial silicon dioxide layer. High-resolution electron beam lithography (EBL using a 100 keV JEOL JBX-9300FS), using a bi-level poly-methyl methacrylate (PMMA) resist, defined the body of the cantilever oscillator. Each sample contained arrays of oscillators. 30 nm of chromium was subsequently deposited using electron beam evaporation and lifted-off in a solution of methylene chloride. Silicon nitride was then etched in a CF_4 plasma using Cr as an etch mask. The Cr was then removed using wet chemical etching and a subsequent O_2 plasma etching. A second, registered, EBL level using a bi-

* Corresponding author.
† School of Applied and Engineering Physics, Nanobiotechnology Center and Cornell Nanofabrication Facility, Cornell University.
‡ School of Electrical and Computer Engineering, Cornell University.
§ Tel Aviv University.

10.1021/nl050456k CCC: $30.25
Published on Web 04/26/2005

layer PMMA resist was performed to define circular openings near the free end of the cantilevers, where the Au dots were to be located. Within each sample, a portion of the fabricated NEMS array was reserved for the evaluation of the selectivity of the binding events, and hence here, Au dots were not defined. Electron beam evaporation of 5 nm of Cr and 15 nm of Au and subsequent lift-off were carried out to define the binding sites. Devices were then released in hydrofluoric acid, rinsed in deionized water, and dried in flowing nitrogen. Figures 1a−c shows optical and scanning electron micrographs of arrays of released oscillators with 40 nm diameter gold contacts.

One factor that strongly affects the resonant frequency shift is the position on the surface of the oscillator where the binding takes place. Controlling the binding location is important for creating devices with a calibrated response to the binding of individual molecules. The maximization in mass sensitivity is achieved through placement of a biomolecular-tethering site at the point where the oscillator's vibrational amplitude is maximum. For a cantilever oscillator, maximum sensitivity is achieved at the free end for the fundamental mode of vibration. To localize the binding site, we formed oscillators, as described above, with nanoscale gold dots at precise locations on the cantilevers to act as spatially and chemically discriminant binding sites to selectively capture disulfide modified dsDNA molecules. Because the bound dsDNA molecule is tethered to the gold nanodot at only one end, we estimated the possible frequency shift variation due to drying in the worst case configurations of the molecules all stretched toward the support end versus stretched in the opposite direction on the cantilever. While a possibly measurable effect, this has no impact on the counting of a few bound molecules.

Both excitation and detection of cantilever motion were performed by scanning laser beams, not requiring precise focusing or alignment with the oscillators. The oscillators therefore can be made much smaller than either the spot size or alignment accuracy of the lasers. We only require that the oscillator spacing be greater than the alignment accuracy and spot size of the detection beam. Measurements were performed with the oscillators in a vacuum chamber that was evacuated to $\sim 3 \times 10^{-7}$ Torr. The out-of-plane motion of the resonators was determined interferometrically by measuring the reflectance variation from a He−Ne laser focused at the free end of the cantilever beam. Reflection from the moving cantilever and the underlying silicon substrate set up a Fabry−Perot cavity. Device motion therefore varied the intensity of the light. Translational stages were used for adjusting the focus and position of the laser beam. The 4 μm laser spot completely covered the nanomechanical oscillator. A spectrum analyzer was used to acquire the modulated output from a photodiode to provide the frequency spectrum of the mechanical response, from which the resonant frequency could be readily extracted.

In the measurement of the resonant devices we used a scanning optical-thermo-mechanical motion excitation method. A chopped laser beam was focused on the surface near the cantilever (Figure 1d). At the resonant frequency of the

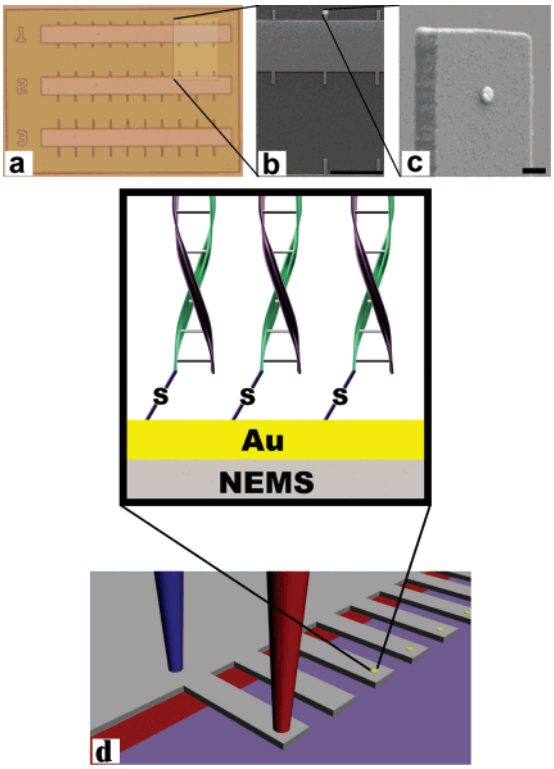

Figure 1. (a) Optical micrograph showing arrays of cantilevers of varying lengths. (b) Zoomed-in scanning electron microscope (SEM) image showing $l = 3.5$ μm, $l = 4.0$ μm, and $l = 5.0$ μm cantilevers. (c) Oblique angle SEM image of the 90 nm thick silicon nitride cantilever with a 40 nm circular Au aperture centered 300 nm away from the free end. Scale bar corresponds to 100 nm. To enhance contrast during imaging, the oscillators were sputter coated with AuPd. (d) Schematic of the optical measurement setup displaying arrays of cantilevers with and without Au dots, as well as the red HeNe and the driving, blue, 415 nm diode laser at the free end and near the periphery of the clamped end, respectively. The top schematic illustrates the binding strategy of the thiolated double stranded DNA molecules to the Au dots near the free end of the cantilevers.

oscillator, thermal waves produced by an intensity modulated 415 nm diode laser excite the motion of the cantilever. The energy of the impinging photons couples into the device layer through localized temperature variations. Since, the thermal conductivity of silicon nitride ($k_{SiN} = 15$ W m^{-1} K^{-1}) is approximately an order of magnitude higher than the underlying layer of silicon dioxide ($k_{SiO2} = 1.4$ W m^{-1} K^{-1}), the heat propagation is accordingly higher in the silicon nitride layer. The resulting temperature gradient induced in the silicon nitride layer is responsible for the inhomogeneous thermal expansion of the cantilever material through the thickness of the cantilever. The thermal stresses necessary for the actuation of the cantilever arise mainly due to the thermal mismatch between the device and silicon dioxide layers rather than to the temperature gradient within the device layer itself. Our calculations show that under resonant excitation with Q-factors on the order of 10^4, the vibrational amplitude can reach levels comparable to the thickness of the sacrificial oxide layer for temperatures much less than one degree. Therefore, the dynamics of the heat transport process can be qualitatively described as injected thermal

energy being carried to the system causing amplified mechanical vibrations.[20]

The location of the driving beam was not critical, and detectable motion could be excited with displacements approaching 50 μm from the cantilever.[20] We could therefore easily scan the exciting beam without critical alignment to activate each cantilever and measure the mechanical response with a second laser. We gave careful consideration to possible thermal effects or nonlinearities influencing the resonant frequency or frequency stability as we want to definitively associate frequency shifts with bound mass. We observed that with optical drive power signals (P_d) less than 14 μW, positioning of the driving laser beam around the periphery of the clamped end of the oscillators did not influence the natural frequency of the nanomechanical device. The onset of nonlinearities could be seen at $P_d \geq 140$ μW and was reminiscent of the behavior previously observed using electrostatic actuation of NEMS devices.[21] With $P_d <$ 14 μW, reproducible measurements of the resonant frequency were achieved with frequency stability of about 10 Hz. Furthermore, we have evaluated frequency stability of driven oscillators with respect to time. In this methodology, the driving beam was placed in close proximity of the clamped end, and out of plane vibrations were monitored over time. These measurements revealed a similar frequency stability of $\sim$10 Hz over a period of 2 h. Similar experiments performed in the moderate nonlinear excitation regime showed chaotic resonant behavior and contact phenomenon. At even higher driving levels, devices were ultimately immobilized through stiction, where the oscillator became attached to the underlying substrate. We thus conclude that the photon induced drive with $P_d <$ 14 μW provides an attractive actuation scheme within which thermal effects do not induce resonant frequency drift.

dsDNA with 5′ thiol modification was used as our model molecular system. The 1587 bp long target dsDNA was produced through polymerase chain reaction (PCR master mix from Brinkmann, Wesyburg, NY). The template used for the production of target dsDNA by PCR was a plasmid vector pVAX1/lacZ (Invitrogen, Carlsbad, CA). The 5′ disulfide-modified forward primer used was R-S-S-GGGAG-GATTGGGAAGACAATAGCA, with the reverse primer being AGCAGCCACTGGTAACAGGATTAG (Integrated DNA Technologies, Coralville, IA). Following the reaction, the primers and the enzyme were then removed with a PCR purification kit (Qiagen Inc, Valencia, CA). The resulting PCR dsDNA product with one disulfide-modified end was then reduced using dithiothreitol immobilized acrylamide resin ("reductacryl", Calniochem. Inc.). The reduction reaction was performed at room temperature for 15 min with agitation. Reduction resin was then removed by centrifugation. The resulting thiol-modified DNA was used immediately following reduction reaction. The target DNA was immobilized onto gold dots (Figure 1d) on the cantilever surface by incubation of 5 ng/μL thiolated dsDNA in 0.1 M NaCl, 10 mM sodium phosphate buffer (pH 7.4) with the cantilever surface at room temperature for 2 h. Later in order to reduce the number of immobilized DNA molecules, we used diluted (0.05 ng/μL) thiolated dsDNA with a 15 min incubation period. After immobilization, an initial rinse followed by a complete immersion of the oscillators in deionized water for a period of 10 min eliminated both the crystallization of the buffer solution as well as the loosely bound DNA molecules on the surface of the oscillators. The samples were then dried with a stream of high purity nitrogen and placed into the vacuum chamber. The resulting frequency spectra were then correlated to the number of immobilized thiolated dsDNA molecules (N_{DNA}).

We carried out systematic binding experiments on more than 100 nanomechanical resonators of varying dimensions. After cantilever array fabrication, initial baseline resonant frequency measurements were made for each oscillator in the array. After binding of the dsDNA, the frequency response of the individual oscillators was measured again. The frequency shift was obtained by fitting a Lorentzian function to the measured data and correlating to the known mass of a single dsDNA molecule ($m_{DNA} = 999$ kDaltons). Our calculations[22] provided the magnitude of the sensitivity of 194, 109, and 54 Hz/ag for cantilevers of $l = 3.5$, 4, and 5 μm, respectively. Furthermore, our calculations take into account the mass location while neglecting the rotational inertia of the attached mass.[22] Verification of the Euler−Bernoulli model was carried out using finite element methods (FEM). Comparison of the results produced by the analytical beam model and the three-dimensional FEM show good agreement.

Control experiments were performed to measure nonspecific binding of material from the buffer solution to the silicon nitride oscillator. For these experiments, we submerged the devices for 2 h in a buffer solution that did not contain DNA molecules. Each device set was composed of arrays of NEMS devices comprised of cantilevers both with and without gold dots. Following the immersion, we thoroughly rinsed the devices in deionized water and dried with pressurized nitrogen. The devices were then measured in the fashion described above. The measured frequency shift revealed the degree of nonspecific binding and its variation between oscillators of different dimensions. Figure 2a is a characteristic spectrum showing a minute change in the natural frequency corresponding to a shift resulting from nonspecific binding of the buffer solution. These characteristic features were reproducible in different sample runs for varying oscillator dimensions. From the specificity experiments, the amount of observed nonspecific binding was 0.26 $\pm$ 0.14 m_{DNA}, 0.44 $\pm$ 0.12 m_{DNA}, and 0.42 $\pm$ 0.09 m_{DNA} for cantilevers of $l = 3.5$, 4, and 5 μm. We have also found that these frequency shifts due to the nonspecific interaction from the control buffer were independent of the presence of the gold dot.

Following control experiments, new devices were immobilized with dsDNA and measured under vacuum. Figure 2b shows characteristic DNA binding spectra indicating an easily resolvable frequency shift corresponding to the mass of 2.04 DNA molecules. During each experiment, binding selectivity of the thiolated DNA to gold was confirmed by measuring the binding response of the functionalized dsDNA

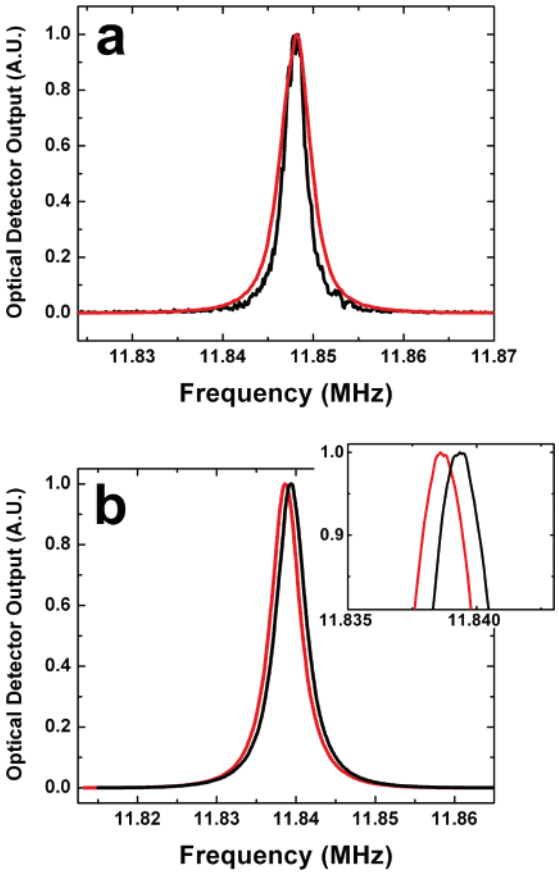

Figure 2. Frequency spectra of the $l = 3.5$ μm oscillators before (black) and after (red) the various stages of binding developed in this study. (a) Control experiment showing a frequency shift corresponding to 0.3 m_{DNA}. (b) Measured frequency spectra resulting from a binding event of ~2.04 DNA molecules. The mechanical quality factor (Q) of these devices ranged from 3000 to 5000.

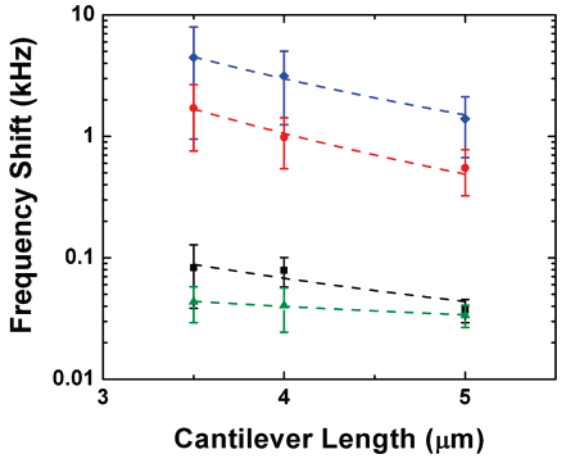

Figure 3. Frequency shift with cantilever length for DNA concentrations of 0.05 ng/μL (red) and 5.0 ng/μL (blue), and control experiments without Au dots (black) and buffer solution without DNA (green). The error bars indicate the standard deviation in the data. Theoretical predictions from FEM simulations show a worst-case scenario of about 15% frequency discrepancy when assuming the DNA molecule perfectly stretched from the Au dot. This probably reflects the continuity of the data when measuring many molecules.

cantilevers without gold dots. In our experiments, only cantilevers with gold dots displayed a frequency shift

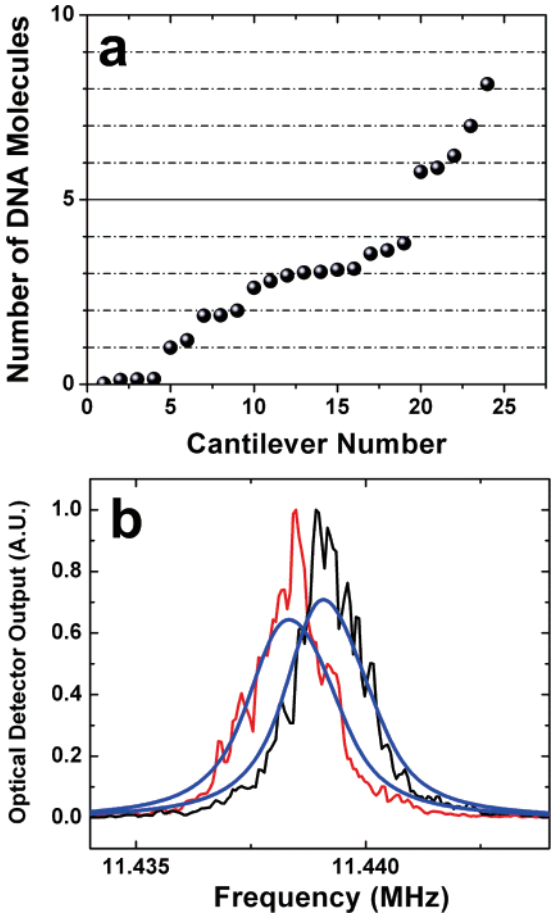

Figure 4. (a) Response of the $l = 3.5$ μm cantilever to the loading effects of 0.03 ng/μL concentration of dsDNA. (b) Frequency spectra before (black) and after (red) the binding events show a frequency shift due to a single dsDNA molecule bound to the Au surface of the cantilever. Enhancement of the mechanical factor (Q~7800) can be attributed to improved vacuum conditions and minimization of outgassing, collectively causing suppressed viscous damping. Even though the data appear rough, the calculated uncertainty from the Lorentzian fit (dashed blue lines) was ±8.33 Hz.

significantly greater than those due to nonspecific binding. NEMS oscillators without Au dots showed a frequency shift of a similar magnitude as seen during control experiments. This lack of binding dependence to devices without gold contacts corroborates excellent binding selectivity of the thiolated dsDNA to the gold nanodots.

Figure 3 illustrates the response of various cantilevers to the mass loading caused by the DNA binding and by the nonspecific binding during control experiments. With the most sensitive cantilever we can detect the binding of a single molecule. For the detection and counting of small numbers of dsDNA molecules, we have utilized cantilevers of lengths $l = 3.5$ μm to sample a 0.03 ng/μL DNA concentration solution for 90 s and 120 s immobilization times (Figure 4).

The substantial and reproducible shift in the natural frequency of individual NEMS strongly suggests that integration of Au dots could be used as specific binding surfaces for a range of biomolecules through the thiol chemistry. Overall, our data indicate that NEMS oscillators with

prefabricated biomolecular tethering sites are good candidates for detection of single biomolecules.

The devices we described are made by lithographic techniques that can form a large number of nearly identical sensing elements in a configuration that integrates well with systems architectures. The optical drive and motion transduction approach allows for rapid interrogation of array elements in a manner similar to conventional binding array technologies. The sensitivity of the devices is sufficient to detect the binding of a single large biomolecule without labeling. Moreover, increased sensitivity would be expected for devices further miniaturized by available high-resolution lithographic methods. Because of the localized binding mass and resulting calibrated response, precise mass quantification can be accomplished for identically immobilized elements and enumeration of discrete bound molecules. Combining the mass detection technique with immunospecific or other optical labeling techniques allows for additional discrimination between different bound compounds. We have incorporated similar mechanical devices in optically accessible microfluidic channels[23] and we anticipate that it is in this configuration that high-resolution nanomechanical sensors would be utilized in diagnostic or sensor systems. Such systems could include the detection of specific sequence analyte DNA in a hybridization array, where nanomechanical elements are functionalized with strands of specified sequences complimentary to those to be detected. The ability to detect a single binding event removes the necessity for PCR amplification. Incorporated micro- and nanofluidic sample delivery and preparation could be utilized for genetic analysis of a single cell. Furthermore, the nanofabricated Au dots can be used as spatially discriminant binding sites for functional proteins, such as antibodies, oligonucleotides, and aptamers for specific detection of target analytes in a complex mixture. The benefits of such tools in research and medical and forensic diagnostics are manifested in a myriad of forms.

Acknowledgment. We acknowledge support for this research from the DARPA and the National Science Foundation through the Nanobiotechnology Center. Device fabrication was done at the Cornell Nanoscale Facility.

References

(1) Ambrose, W. P.; Goodwin, P. M.; Martin, J. C.; Keller, R. A. *Phys. Rev. Lett.* **1994**, *72*, 160.
(2) Kneipp, K.; et al. *Phys. Rev. Lett.* **1997**, *78*, 1667.
(3) Rief, M.; Oesterhelt, F.; Heymann, B.; Gaub, H. E. *Science* **1997**, *275*, 1295.
(4) Rief, M.; Clausen-Schaumann, H.; Gaub, H. E. *Nat. Struct. Biol.* **1999**, *6*, 346.
(5) Hugel, T.; et al. *Science* **2002**, *296*, 1103.
(6) Bustamante, C.; Bryant, Z.; Smith, S. B.; *Nature* **2003**, *421*, 423.
(7) Levine, M.; et al. *Science* **2003**, *299*, 682.
(8) Craighead, H. G. *Science* **2000**, *290*, 1532.
(9) Thundat, T.; et al. *Appl. Phys. Lett.* **2000**, *77*, 4061, 2000.
(10) Hu, Z.; Thundat, T.; Warmack, R. J. *J. Appl. Phys.* **2001**, *90*, 427.
(11) Fritz, J.; et al. *Science* **2000**, *288*, 316.
(12) Ilic, B.; et al. *Appl. Phys. Lett.* **2000**, *77*, 450.
(13) Lavrik, N. V.; Sepaniak, M. J.; Datskos, P. G. *Rev. Sci. Instrum.* **2004**, *75*, 2229.
(14) Földes-Papp, Z.; Demel, U.; Tilz, G. P. *Proc. Natl. Acad. Sci. U.S.A.* **2001**, *98*, 11509.
(15) Cotlet, M.; et al. *Proc. Natl. Acad. Sci. U.S.A.* **2001**, *98*, 14398.
(16) Williams, P. A.; et al. *Phys. Rev. Lett.* **2002**, *89*, 255502.
(17) Qian, D.; Wagner, G. J.; Liu, W. K.; Yu, M.-F.; Ruoff, R. S. *Appl. Mech. Rev.* **2002**, *55*, 495.
(18) Papadakis, S. J., et al. *Phys. Rev. Lett.* **2004**, *93*, 146101.
(19) Sazonova, V. et al. *Nature* **2004**, *431*, 284.
(20) Ilic, B.; Krylov, S.; Aubin, K.; Reichenbach, R.; Craighead, H. G.; accepted for publication in *Appl. Phys. Lett*.
(21) Carr, D. W.; Evoy, S.; Sekaric, L.; Craighead, H. G.; Parpia, J. M. *Appl. Phys. Lett.* **1999**, 75, 920.
(22) Ilic, B.; et al. *J. Appl. Phys.* **2004**, *95*, 3694.
(23) Czaplewski, D.; et al. *J. Microelectromech. Syst.* **2004**, *13*, 576.

NL050456K